Cellular/Molecular

Compartmentalization of the $GABA_B$ Receptor Signaling Complex Is Required for Presynaptic Inhibition at Hippocampal Synapses

Tal Laviv,[1] Irena Vertkin,[1] Yevgeny Berdichevsky,[1] Hilla Fogel,[1] Inbal Riven,[1] Bernhard Bettler,[3] Paul A. Slesinger,[2] and Inna Slutsky[1]

[1]Department of Physiology and Pharmacology, Sackler Faculty of Medicine, Tel Aviv University, 69978 Tel Aviv, Israel, [2]Peptide Biology Laboratory, The Salk Institute for Biological Studies, La Jolla, California 92037, and [3]Department of Biomedicine, Institute of Physiology, Pharmazentrum, University of Basel, CH-4056 Basel, Switzerland

Presynaptic inhibition via G-protein-coupled receptors (GPCRs) and voltage-gated Ca^{2+} channels constitutes a widespread regulatory mechanism of synaptic strength. Yet, the mechanism of intermolecular coupling underlying GPCR-mediated signaling at central synapses remains unresolved. Using FRET spectroscopy, we provide evidence for formation of spatially restricted (<100 Å) complexes between $GABA_B$ receptors composed of GB_{1a}/GB_2 subunits, $G\alpha_o\beta_1\gamma_2$ G-protein heterotrimer, and $Ca_V2.2$ channels in hippocampal boutons. GABA release was not required for the assembly but for structural reorganization of the precoupled complex. Unexpectedly, GB_{1a} deletion disrupted intermolecular associations within the complex. The GB_{1a} proximal C-terminal domain was essential for association of the receptor, $Ca_V2.2$ and $G\beta\gamma$, but was dispensable for agonist-induced receptor activation and cAMP inhibition. Functionally, boutons lacking this complex-formation domain displayed impaired presynaptic inhibition of Ca^{2+} transients and synaptic vesicle release. Thus, compartmentalization of the $GABA_{B1a}$ receptor, $G\beta\gamma$, and $Ca_V2.2$ channel in a signaling complex is required for presynaptic inhibition at hippocampal synapses.

Introduction

G-protein-coupled receptors (GPCRs), G-proteins, and N- and P/Q-type high-voltage-gated Ca^{2+} (Ca_V) channels (Nowycky et al., 1985) represent key signaling elements controlling Ca^{2+} flux at nerve terminals (Dunlap et al., 1995). Since the first work of Dunlap and Fischbach (1978), numerous studies suggest that GPCR activation induces inhibition of Ca_V channels via direct interaction with $G\beta\gamma$ subunits of G-proteins (for review, see Hille, 1994; Zamponi and Snutch, 1998; Catterall, 2000; Dolphin, 2003; De Waard et al., 2005). This membrane-delimited mechanism of Ca_V channel inhibition has been proposed to enable precise inhibition of neurotransmitter release in space and time.

Despite several decades of intensive research, the intermolecular coupling mechanism underlying GPCR-mediated presynaptic inhibition at central synapses remains unresolved. According to collision coupling theory assuming free lateral diffusion of receptors, G-proteins, and effectors within the cell membrane, only receptors activated by agonist are capable of interacting with G-proteins (Orly and Schramm, 1976; Tolkovsky and Levitzki, 1978). As this model encounters difficulty explaining signaling specificity at the single-cell level, alternative models were proposed that assume coupling between the signaling units without agonist (precoupling) and formation of predetermined signaling microdomains (Neubig et al., 1988; Neubig, 1994). However, currently there is no experimental evidence supporting any of these models in central synapses.

Recent advances in molecular biology and optical imaging enabled real-time monitoring of intermolecular dynamics in living cells by resonance energy transfer technology (Lohse et al., 2008). These studies in heterologous expression systems, although boosting our understanding of receptor/G-protein/effector coupling mechanisms, yielded conflicting results. Some studies have suggested existence of precoupled complexes between GPCRs, G-proteins, and effectors such as G-protein-activated inwardly rectifying K^+ (GIRK) channels (Nobles et al., 2005; Galés et al., 2006; Riven et al., 2006; Fowler et al., 2007), and diffusion-determined collision coupling has been proposed by others (Hein et al., 2005). The disparity between these results emphasizes the need to study intermolecular dynamics in native environments and at specialized subcellular compartments.

Among various presynaptic GPCRs, $GABA_B$ receptors are widely expressed in the brain as autoreceptors and heteroreceptors (Wu and Saggau, 1997; Bettler et al., 2004). $GABA_B$ receptors

Received March 25, 2011; revised July 5, 2011; accepted July 11, 2011.

Author contributions: T.L., I.V., P.A.S., and I.S. designed research; T.L., I.V., Y.B., H.F., and I.R. performed research; B.B. and P.A.S. contributed unpublished reagents/analytic tools; T.L., I.V., H.F., I.R., and I.S. analyzed data; T.L., P.A.S., and I.S. wrote the paper.

This work was supported by the Israel Science Foundation (I.S., Grants 993/08, 1925/08 and 170/08), the Binational Science Foundation (I.S. and P.A.S., Grant 2007199), and the Swiss Science Foundation (3100A0–117816). We thank Dr. N. Dascal and Dr. E. Reuveny for helpful discussions; Dr. E. Reuveny for providing $TNFR_2^{YFP}$, $G\beta_1^{YFP}$, and $G\gamma_2^{YFP}$ cDNAs; and Dr. K. Jalink for providing CFP-Epak-YFP cDNA.

Correspondence should be addressed to Dr. Inna Slutsky, Sackler Faculty of Medicine, Department of Physiology and Pharmacology, Tel Aviv University, Ramat Aviv, Tel Aviv 69978, Israel. E-mail: islutsky@post.tau.ac.il.

I. Riven's present address: Department of Chemical Physics, Weizmann Institute of Science, 76100 Rehovot, Israel.

DOI:10.1523/JNEUROSCI.1527-11.2011

 0270-6474/11/3112523-10$15.00/0

are obligatory heterodimers, requiring two homologous subunits, GB_1 and GB_2, to function (Jones et al., 1998; Kaupmann et al., 1998; White et al., 1998; Kuner et al., 1999). Molecular diversity of $GABA_B$Rs arises from two pharmacologically indistinguishable GB_1 isoforms, 1a and 1b (Bettler et al., 2004), and from auxiliary KCTD subunits (Schwenk et al., 2010). Transgenic mice with targeted isoform-specific genetic deletions suggest that GB_{1a}-containing receptors (GB_{1a}Rs) are predominantly localized at glutamatergic boutons, mediating presynaptic inhibition of glutamate release (Vigot et al., 2006; Guetg et al., 2009). Activation of presynaptic $GABA_B$ receptors induces inhibition of synaptic vesicle release through suppression of Ca^{2+} flux (Wu and Saggau, 1995; Takahashi et al., 1998; Laviv et al., 2010), although several Ca^{2+}-independent mechanisms have been proposed as well (Scanziani et al., 1992; Parnas et al., 2000; Sakaba and Neher, 2003). Recent quantitative proteomic study on molecular composition of Ca_V2 channel nano-environment suggests that $GABA_B$ receptors strongly interact with $Ca_V2.2$ channels in the brain (Müller et al., 2010).

Although much information has been gained on the structure and function of $GABA_B$ receptors, several key questions remain unresolved. First, does assembly of the presynaptic GB_{1a}R–G$\beta\gamma$–$Ca_V2.2$ complex require synaptic activity or, alternatively, are the signaling units precoupled in a macromolecular complex regardless of GABA-induced activation? Second, how does GABA affect the microarchitecture of signaling complexes at individual synaptic boutons? Third, are GB_{1a}Rs required for the complex formation? And finally, if GB_{1a}Rs are indeed compartmentalized with G$\beta\gamma$ subunits and $Ca_V2.2$ channels, how does it impact the function of central synapses? To address these questions, we integrated fluorescence resonance energy transfer (FRET) spectroscopy, optical imaging of vesicle exocytosis, and presynaptic calcium transients at individual presynaptic boutons in cultured hippocampal neurons (Laviv et al., 2010). Our findings suggest that GB_{1a}Rs, G-protein heterotrimers and $Ca_V2.2$ channels are precoupled in presynaptic hippocampal boutons. We identified the proximal C-terminal domain of the GB_{1a} protein as an essential molecular domain mediating the GB_{1a}R–G$\beta\gamma$–$Ca_V2.2$ signaling complex assembly but as dispensable for the receptor and $G\alpha_{i/o}$ activation. The structural segregation of ligand-binding and complex-formation domains allowed us to isolate the impact of signaling compartmentalization on presynaptic function. Our findings suggest that ligand-induced receptor activation is necessary but insufficient for presynaptic inhibition and propose that precoupling of GB_{1a}Rs, G$\beta\gamma$ subunits, and $Ca_V2.2$ channels in a signaling nano-domain is required for a proper negative regulation of basal synaptic vesicle release at hippocampal synapses.

Materials and Methods

Hippocampal cell culture. Primary cultures of CA3-CA1 hippocampal neurons were prepared from newborn Wistar rats and $1a^{-/-}$, $1b^{-/-}$, WT (BALB/c background) mice on postnatal days 0–2, as described previously (Slutsky et al., 2004). The generation of the $1a^{-/-}$ and $1b^{-/-}$ mice has been described previously (Vigot et al., 2006). All animal experiments were approved by the Tel Aviv University Committee on Animal Care.

Molecular biology. Construction of fusion proteins has been described previously: GB_{1a}^{CFP}, GB_{1a}^{YFP}, and $G\alpha_o^{CFP}$ (Fowler et al., 2007); pHluorin-GB_{1a} (Guetg et al., 2009); $G\beta_1^{YFP}$, $G\gamma_2^{CFP}$ (Riven et al., 2006); CFP-Epak-YFP (van der Krogt et al., 2008); and $Ca_V2.2^{CFP}$ (Altier et al., 2006). Wild type and mutants of GB_{1a} proteins used throughout the study were constructed and expressed in peYFP-N1 under control of CMV promoter. Nontagged GB_{1a}-WT protein was engineered by digestion of peYFP-N1-GB_{1a}-WT with AgeI/NotI, and then blunting and religation. GB_{1a}-Δ21-YFP was created by overlap-extension PCR and subcloning into peYFP-N1-GB_{1a}-WT using BamHI/AgeI. Nontagged GB_{1a}-Δ21 was created by digestion peYFP-N1-GB_{1a}-Δ21 with AgeI/NotI, and then blunting and religation. Nontagged GB_{1a}-ΔSD receptor was engineered by overlap-extension PCR and subcloning into EcoRI/BamHI sites of peYFP-N1 plasmid bearing the nontagged GB_1a-WT receptor gene. GB_{1a}-S269A-YFP was created by overlap-extension PCR and subcloning into ApaI/AgeI sites of peYFP-N1-GB_{1a}-WT. Nontagged GB_{1a}-S269A was constructed by digestion of peYFP-N1-GB_{1a}-S269A with AgeI/NotI, and then blunting and religation. Nontagged GB_{1a}-Δ103 was created by PCR and then subcloned into BamHI/NotI sites of peYFP-N1-GB_{1a}-WT. Nontagged GB_{1a}-Δ74 and GB_{1a}-Δ39 were described previously (Boyer et al., 2009).

Transient cDNA transfections have been performed using Lipofectamine-2000 reagents and neurons were typically imaged 18–24 h after transfection.

Confocal imaging. Hippocampal neurons were imaged using a Zeiss LSM510 META confocal microscope (Carl Zeiss) using a 40 × 1.2 NA water-immersion objective and FV1000 spectral Olympus confocal microscope using a 60 × 1.2 NA water-immersion objective. The experiments were conducted at room temperature in extracellular Tyrode solution containing the following (in mM): NaCl, 145; KCl, 3; glucose, 15; HEPES, 10; $MgCl_2$, 1.2; $CaCl_2$, 1.2; pH adjusted to 7.4 with NaOH. To isolate miniature synaptic activity, TTX (1 μM) was added to extracellular solution.

FRET imaging. FRET imaging was carried as described previously (Laviv et al., 2010). For spectral analysis, CFP was excited at 405 nm (Zeiss) or at 442 nm (Olympus) and fluorescence emission was measured between 400 and 700 nm, with a 10 nm λ step size. To reduce phototoxicity and photobleaching, most of the FRET experiments were performed using a narrowed emission spectrum (460–560 nm) composed of CFP peak (486 ± 10 nm) and a YFP peak (534 ± 10 nm) containing YFP emission due to FRET, direct YFP excitation at 405 nm, and CFP emission tail. YFP was imaged at 514 nm (excitation) and 525–560 nm (emission). Photobleaching of YFP was performed with 514 nm laser line, at 2.3 mW of laser output. We used a single point activation module for rapid and efficient multiregion bleaching. We typically photobleached two to six boutons per imaged axon: bleach duration was 35 ms per bouton with a 5 ms interval between boutons.

Image acquisition parameters were optimized for maximal signal-to-noise ratio and minimal phototoxicity: 700 V photomultiplier voltage; 4 μs/pixel scan speed, 0.05–0.18 mW (514 nm) or 0.15–0.2 (440 nm) laser output; 90–130 μm pinhole; 512 × 512 pixels image size. *Z*-stacks were collected from 3–4 μm optical slice at 0.6–0.8 μm steps; images were then stacked using maximal intensity projection per pixel algorithm and converted to a single 2D image for analysis. Images were acquired without averaging.

Calculation of FRET efficiency. Donor dequenching due to the desensitized acceptor was measured from CFP emission (460–500 nm) before and after the acceptor photobleaching. FRET efficiency, *E*, was then calculated using the equation $E = 1 - I_{DA}/I_D$, where I_{DA} is the peak of donor emission in the presence of the acceptor and I_D is the peak after acceptor photobleaching. To exclude potential contribution of donor/acceptor ratio to FRET efficiency measurements, all FRET experiments were performed under saturation conditions of acceptor over donor. Detection of CFP/YFP signals was done using custom-written scripts in MATLAB (MathWorks) as described previously (Laviv et al., 2010). Briefly, regions of interest (ROIs) were marked at boutons that underwent YFP photobleaching. Average intensity of ROIs was subtracted from background ROI intensity in close proximity to the bouton. All the boutons that exhibited YFP photobleaching by >90% of initial fluorescence intensity were included in the analysis. Nonbleached boutons at the same image area were analyzed to ensure lack of nonspecific photobleaching due to image acquisition.

Detecting presynaptic calcium transients. Fluorescent calcium indicator Calcium Green 488 BAPTA-1 AM was dissolved in DMSO to yield a concentration of 1 mM. For cell loading, cultures were incubated at 37°C for 30 min with 3 μM of this solution diluted in standard extracellular

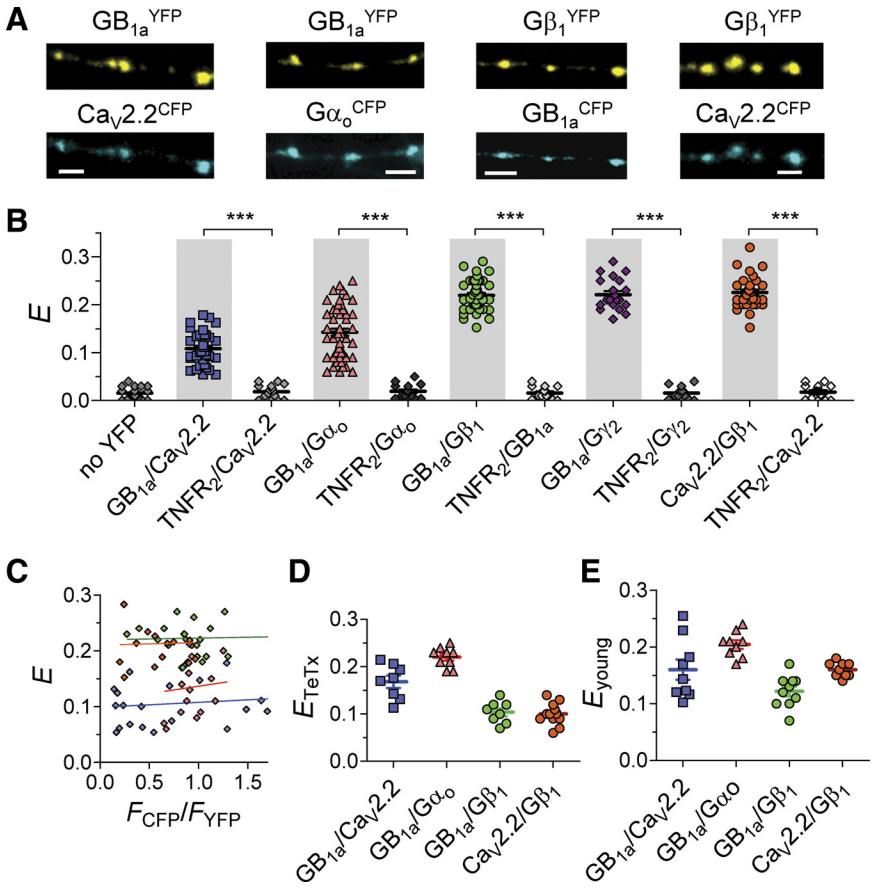

Figure 1. $GB_{1a}Rs$, $G\alpha_o\beta_1\gamma_2$ G-protein subunits, and $Ca_V2.2$ channels are precoupled at single hippocampal boutons. ***A***, Representative confocal images of pyramidal neuron axons in hippocampal cultures that were cotransfected with $GB_{1a}^{YFP}/Ca_V2.2^{CFP}$, $GB_{1a}^{YFP}/G\alpha_o^{CFP}$, $GB_{1a}^{CFP}/G\beta_1^{YFP}$ and $Ca_V2.2^{CFP}/G\beta_1^{YFP}$. Scale bars, 2 μm. ***B***, FRET was detected between $GB_{1a}^{YFP}/Ca_V2.2^{CFP}$ ($n = 33, N = 7$), $GB_{1a}^{YFP}/G\alpha_o^{*94CFP}$ ($n = 53$), $GB_{1a}^{CFP}/G\beta_1^{YFP}$ ($n = 45, N = 10$), $GB_{1a}^{CFP}/G\gamma_2^{YFP}$ ($n = 21, N = 4$), $Ca_V2.2^{CFP}/G\beta_1^{YFP}$ ($n = 31, N = 6$) proteins under miniature synaptic activity at single hippocampal boutons. To verify FRET specificity, *E* was measured between the CFP-tagged proteins of interest and nonrelated $TNFR_2^{YFP}$. Error bars indicate SEM. ***$p < 0.001$. ***C***, FRET efficiency is plotted for individual presynaptic boutons as function of CFP/YFP intensity ratio (F_{CFP}/F_{YFP}). No correlation was found: Spearman *r* is 0.14, 0.11, −0.08, and 0.05 for $GB_{1a}^{YFP}/Ca_V2.2^{CFP}$, $GB_{1a}^{YFP}/G\alpha_o^{*94CFP}$, $GB_{1a}^{CFP}/G\beta_1^{YFP}$, and $Ca_V2.2^{CFP}/G\beta_1^{YFP}$, respectively ($p > 0.5$). ***D***, FRET was detected between $GB_{1a}^{YFP}/Ca_V2.2^{CFP}$ ($n = 8, N = 3$), $GB_{1a}^{YFP}/G\alpha_o^{CFP}$ ($n = 9, N = 3$), $GB_{1a}^{CFP}/G\beta_1^{YFP}$ ($n = 8, N = 3$), and $Ca_V2.2^{CFP}/G\beta_1^{YFP}$ ($n = 12, N = 4$) proteins in nonreleasing TeTx-pretreated hippocampal boutons. ***E***, FRET was detected between $GB_{1a}^{YFP}/Ca_V2.2^{CFP}$ ($n = 9, N = 3$), $GB_{1a}^{YFP}/G\alpha_o^{CFP}$ ($n = 9, N = 3$), $GB_{1a}^{CFP}/G\beta_1^{YFP}$ ($n = 10, N = 3$), and $Ca_V2.2^{CFP}/G\beta_1^{YFP}$ ($n = 9, N = 3$) proteins in nonreleasing immature (4–5 DIV) hippocampal neurons.

solution. Extracellular solution contained 20 μM DNQX to block recurrent activity and 50 μM APV to block calcium flux through NMDA receptors. Imaging was performed using FV1000 Olympus confocal microscope, under 488 nm (excitation) and 510–570 nm (emission), using 500 Hz line scanning. Ca^{2+} transients were quantified following averaging of 10 traces. Integral was calculated for $\Delta F/F$ per bouton before and after baclofen application. Integration time window was 300 ms, starting from the end of the stimulus.

FM-based imaging and analysis. Activity-dependent FM1-43 and FM4-64 styryl dyes have been used to estimate basal synaptic vesicle exocytosis. Action potentials have been elicited by passing 50 mA constant current for 1 ms (~50% above the threshold for eliciting action potential) through two platinum wires, separated by ~7 mm and close to the surface of the coverslip. The extracellular medium contained nonselective antagonist of ionotropic glutamate receptors (kynurenic acid, 0.5 mM) to block recurrent neuronal activity. Synaptic vesicles were loaded with 15 μM FM4-64 in all the experiments with GFP/CFP/YFP transfection, and 10 μM FM1-43 was used in all the nontransfected neurons. FM was loaded by bathing the cultures in a medium containing dye. FM was present 5 s before and 30 s after the electrical stimulation (600 stimuli at 20 Hz). After dye loading, external dye was washed away in Ca^{2+}-free solution containing ADVASEP-7 (0.1 mM) to scavenge membrane-bound FM. The fluorescence of individual synapses was determined from the difference between images obtained after staining and after destining (ΔF). For detection of FM^+ puncta, ΔF images have been analyzed (only the puncta exhibiting ≥90% destaining were subjected to analysis). Detection of signals has been done using custom-written scripts in MATLAB as described previously (Abramov et al., 2009). Briefly, the following criteria were used for signal detection: the fluorescence intensity was 2 SDs above the mean background and the area of puncta was between 0.1 and 2 μm^2.

Chemical reagents. FM4-64 (SynaptoRed C2), FM1-43 (SynaptoGreen C4), and Advasep-7 were purchased from Biotium; baclofen, DNQX, CGP35348, and CGP54626 from Tocris Bioscience; TTX from Alomon Labs; TeTx, APV, and kynurenic acid from Sigma-Aldrich; and PTX from Calbiochem.

Statistical analysis. Error bars shown in the figures represent SEM. The number of boutons is defined by *n* and the number of experiments (cultures) by *N*. All the experiments were repeated at least in three different batches of cultures. One-way ANOVA with *post hoc* Dunnett's or Bonferroni's tests was used to compare several conditions. Student's unpaired *t* tests were used in the experiments where two populations of synapses were compared. Student's paired *t* tests were used when the same population of synapses was tested before and after treatment. *$p < 0.05$; **$p < 0.01$; ***$p < 0.001$; n.s., nonsignificant.

Results

$GABA_BRs$, G-proteins, and $Ca_V2.2$ channels are precoupled at hippocampal boutons

In presynaptic terminals, the $GABA_BR$ is a heterodimer of GB_{1a}/GB_2 subunits that mediates GABA-dependent inhibition of voltage-gated N-type Ca channels (Wu and Saggau, 1995; Dittman and Regehr, 1996). Inhibition of $Ca_V2.2$ channels occurs through a G-protein-dependent mechanism (Takahashi et al., 1998). Using FRET to detect intermolecular associations between CFP/YFP-tagged proteins, we examined whether presynaptic $GABA_B$ receptors interact with $Ca_V2.2$ channels and G-proteins at individual hippocampal boutons. We investigated possible associations between $GB_{1a}Rs$, $G\alpha_o\beta_1\gamma_2$ G-protein subunits, and $Ca_V2.2$ channels at boutons of pyramidal hippocampal neurons using the following tagged proteins (Fig. 1*A*): (1) YFP-tagged GB_{1a} receptor subunit (GB_{1a}^{YFP}) (Fowler et al., 2007); (2) CFP-tagged α_1 subunit of $Ca_V2.2$ channel ($Ca_V2.2^{CFP}$) (Altier et al., 2006); (3) CFP-tagged $G\alpha_o$ subunit, where CFP is internally inserted after E94 ($G\alpha_o^{CFP}$) (Fowler et al., 2007); (4) $G\beta_1$ G-protein subunit N-terminally tagged to YFP ($G\beta_1^{YFP}$) (Riven et al., 2006); and (5) $G\gamma_2$ G-protein subunit N-terminally tagged to YFP ($G\gamma_2^{YFP}$) (Riven et al., 2006). All of the tagged proteins were functionally characterized previously (Altier et al., 2006; Riven et al., 2006; Fowler et al., 2007; Laviv et al., 2010). Presynaptic localization of tagged $GABA_B$ receptors in boutons was confirmed previously by colocalization of GB_{1a}^{YFP} with CFP-tagged synapsin Ia protein and with FM4-64 dye (Laviv

et al., 2010). We first examined the basal FRET efficiency (E), determined by donor (CFP) dequenching following acceptor (YFP) photobleaching (Laviv et al., 2010), produced by spontaneous miniature synaptic activity in the presence of tetrodotoxin (+TTX). We detected significant FRET efficiencies between $GB_{1a}^{YFP}/Ca_V2.2^{CFP}$ (0.11 ± 0.006, $n = 33$), $GB_{1a}/G\alpha_o^{94CFP}$ (0.14 ± 0.007, $n = 53$), $GB_{1a}^{CFP}/G\beta_1^{YFP}$ (0.22 ± 0.005, $n = 45$), $GB_{1a}^{CFP}/G\gamma_2^{YFP}$ (0.22 ± 0.007, $n = 21$), and $Ca_V2.2^{CFP}/G\beta_1^{YFP}$ (0.22 ± 0.006, $n = 31$). On average, FRET efficiencies for all the tested protein pairs were significantly higher ($p < 0.0001$, mean E varied from 0.12 to 0.23 between the pairs) than nonspecific FRET between CFP-tagged proteins of interest and a nonrelated tumor necrosis factor receptor 2, C-terminally tagged with YFP ($TNFR_2^{YFP}$) (<2%) (Fig. 1*B*). Furthermore, background enhancement of CFP emission, assessed by photobleaching at 514 nm in neurons expressing only GB_{1a}^{CFP}, was negligible (0.016 ± 0.002, $n = 26$) (Fig. 1*B*). FRET efficiency did not depend on the donor-to-acceptor ratio (Fig. 1*C*). Therefore, FRET measurements suggest close association of the receptor and G-proteins ($GB_{1a}/G\alpha_o^{94CFP}$; $GB_{1a}^{CFP}/G\beta_1^{YFP}$; $GB_{1a}^{CFP}/G\gamma_2^{YFP}$), the channel and G-proteins ($Ca_V2.2^{CFP}/G\beta_1^{YFP}$) and, interestingly, between the receptor and channel ($GB_{1a}^{YFP}/Ca_V2.2^{CFP}$), in hippocampal boutons under miniature synaptic activity.

To assess whether miniature synaptic activity is required for induction of $GB_{1a}R$–G-protein–$Ca_V2.2$ channel associations, we examined FRET efficiencies within the tagged proteins of interest under resting conditions in boutons that are incapable of vesicle recycling and, therefore, lack vesicular GABA release. To accomplish this, we measured FRET in tetanus toxin (TeTx) treated neurons, in which SNARE-mediated vesicle release is inhibited (Fig. 1*D*) and in immature boutons of young (4–5 DIV) neurons (Fig. 1*E*). Notably, basal FRET increased by ~50% between $GB_{1a}^{YFP}/G\alpha_o^{CFP}$ ($p < 0.01$) and $GB_{1a}^{YFP}/Ca_V2.2^{CFP}$ ($p < 0.05$), and it decreased by ~45% between $GB_{1a}^{CFP}/G\beta_1^{YFP}$ ($p < 0.0001$) and by ~35% between $Ca_V2.2^{CFP}/G\beta_1^{YFP}$ ($p < 0.001$) proteins in both young and TeTx-treated neurons. Together, these data suggest that (1) GB_{1a}, $G\alpha_o\beta_1g_2$ G-protein, and $Ca_V2.2$ channel are preassembled in the absence of GABA release; and (2) miniature GABA release triggers rearrangement in the signaling complex, promoting FRET between precoupled $GB_{1a}/G\beta_1g_2$ and $Ca_V2.2/G\beta_1$ proteins, while reducing FRET between the $GB_{1a}/Ca_V2.2$ channel and $GB_{1a}/G\alpha_o$ proteins.

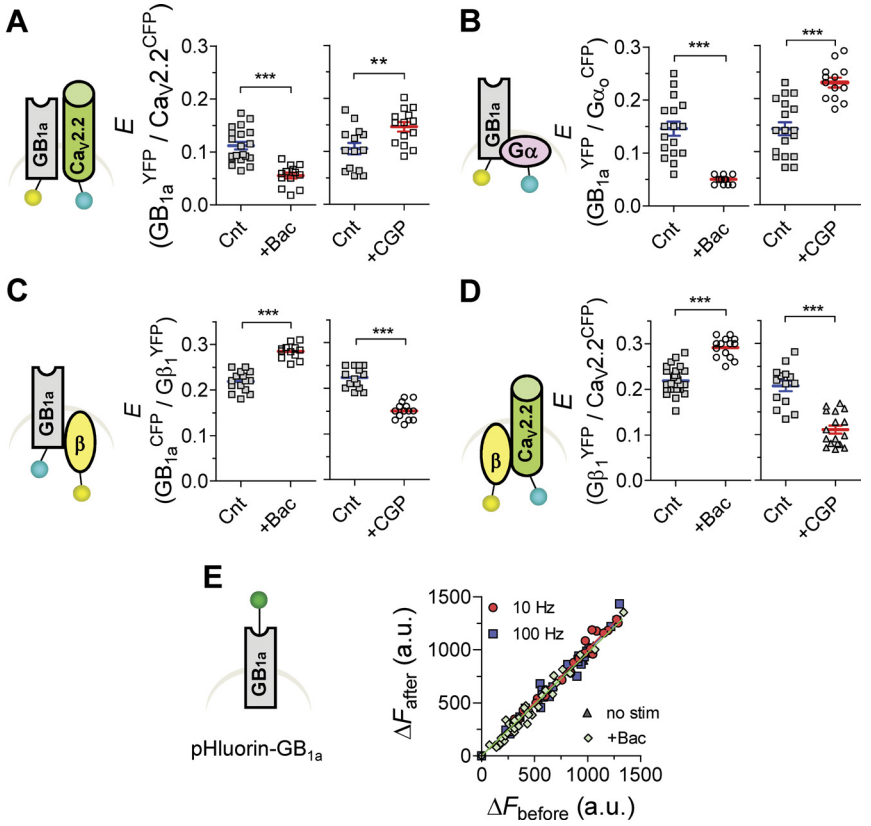

Figure 2. Agonist-induced structural rearrangements in the $GB_{1a}R$/G-protein/$Ca_V2.2$ channel complex. ***A***, E between $GB_{1a}^{YFP}/Ca_V2.2^{CFP}$ was reduced by baclofen (10 μM, left, $n = 13–29$, $N = 4–6$, $^{***}p < 0.0001$), but was increased by CGP54626 (1 μM, right, $n = 14$, $N = 4$, $^{**}p < 0.01$). ***B***, E between $GB_{1a}^{YFP}/G\alpha_o^{CFP}$ was reduced by baclofen (10 μM, left, $n = 12–17$, $N = 4$, $^{***}p < 0.0001$), but was increased by $GABA_BR$ antagonist CGP35348 (1 μM, right, $n = 13–18$, $N = 4$, $^{***}p < 0.0001$). ***C***, E between $GB_{1a}^{CFP}/G\beta_1^{YFP}$ was increased by baclofen (10 μM, left, $n = 12–15$, $N = 4$, $^{***}p < 0.0001$), but was decreased by $GABA_BR$ antagonist CGP54626 (1 μM, right, $n = 15$, $N = 4$, $^{***}p < 0.0001$). ***D***, E between $G\beta_1^{YFP}/Ca_V2.2^{CFP}$ was increased by baclofen (10 μM, left, $n = 14–27$, $N = 4–6$, $^{***}p < 0.0001$), but was decreased by CGP54626 (1 μM, right, $n = 14–17$, $N = 4–5$, $^{***}p < 0.0001$). Error bars indicate SEM. ***E***, Fluorescence intensity of pHluorin tagged to GB_{1a} does not change under miniature activity, by application of 10 μM baclofen and as function of stimulation frequency (10 and 100 Hz). Slope of linear fit is 1.04, 0.98, 1.01, and 0.99 for miniature activity, baclofen application, 10 and 100 Hz, respectively.

Agonist-induced rearrangements within the $GB_{1a}R$ signaling complex

To further assess activity-dependent intermolecular conformational changes within the $GB_{1a}R$ signaling complex, we explored effects of $GABA_BR$ agonist and antagonist on FRET between the tested protein pairs. For the receptor and channel, FRET between GB_{1a}^{YFP} and $Ca_V2.2^{CFP}$ proteins decreased by ~60% following application of 10 μM baclofen ($n = 13–20$, $p < 0.0001$) (Fig. 2*A*, left). Conversely, the $GABA_B$ receptor antagonist CGP54626 (1 μM) triggered a ~40% increase in $GB_{1a}^{YFP}/Ca_V2.2^{CFP}$ FRET ($n = 14$, $p < 0.01$) (Fig. 2*A*, right). CGP54626 did not affect E in the absence of neurotransmitter release ($n = 8$, $p > 0.6$). We next examined the effect of pertussis toxin (PTX), which uncouples the $G\alpha_{i/o}$ subunit from the receptor. Baclofen did not alter FRET between $GB_{1a}^{YFP}/Ca_V2.2^{CFP}$ proteins in PTX-treated neurons (0.12 ± 0.012 vs 0.115 ± 0.011 for control and PTX-treated neurons, respectively, $n = 7–8$, $p > 0.8$), indicating functional coupling with the receptor was required for baclofen effect. For the receptor and G-protein, baclofen significantly decreased $GB_{1a}^{YFP}/G\alpha_o^{CFP}$ FRET (0.05 ± 0.002, $n = 12$, $p < 0.0001$) (Fig. 2*B*, left), similar to a previous study (Frank et al., 2005). Pretreatment with PTX abolished baclofen-induced FRET changes (0.13 ± 0.013 vs 0.14 ± 0.02 for control and PTX-treated neurons, respectively, $n = 13$, $p > 0.2$). CGP35348 (1 μM) induced a ~70% increase in FRET (0.23 ± 0.009, $n = 13$, $p < 0.0001$) (Fig. 2*B*, right) but had no effect in the absence of neurotransmitter release ($n = 8–16$, $p > 0.4$). Together, these data suggest that quantal GABA release weakens association between precoupled $Ca_V2.2$ channel/GB_{1a} receptor subunit and $GB_{1a}/G\alpha_o$ proteins.

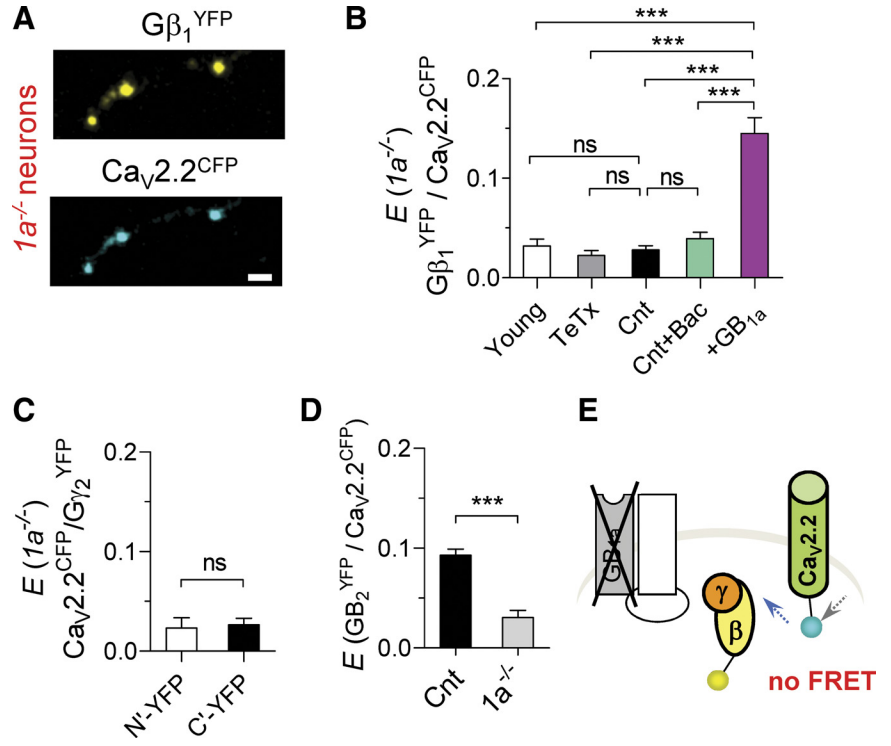

Figure 3. Disruption of FRET between the receptor, $Ca_V2.2$ channel, and $G\beta\gamma$ at hippocampal boutons of $1a^{-/-}$ neurons. ***A***, Confocal images of axonal part of $1a^{-/-}$ hippocampal pyramidal neuron that was cotransfected with $Ca_V2.2^{CFP}$ and $G\beta_1^{YFP}$. Scale bar, 2 μm. ***B***, Lack of specific FRET between $Ca_V2.2^{CFP}$ and $G\beta_1^{N'\text{-}YFP}$ in $1a^{-/-}$ boutons: under miniature synaptic activity (Cnt, $n = 31$, $N = 6$), in the presence of 10 μM baclofen ($n = 16$, $N = 4$), and in TeTx-treated ($n = 14$, $N = 3$) and young ($n = 14$, $N = 4$) neurons. Transfection of $1a^{-/-}$ neurons with GB_{1a} resulted in rescue of $Ca_V2.2^{CFP}/G\beta_1^{N'\text{-}YFP}$ FRET ($n = 17$, $N = 4$, ***$p < 0.0001$). ***C***, Lack of specific FRET between $Ca_V2.2^{CFP}$ and either $G\gamma_2^{N'\text{-}YFP}$ ($n = 10$, $N = 3$) or $G\gamma_2^{C'\text{-}YFP}$ ($n = 9$, $N = 3$). ***D***, Disruption of specific FRET between $Ca_V2.2^{CFP}$ and GB_2^{YFP} protein in $1a^{-/-}$ neurons ($n = 8$, $N = 3$, ***$p < 0.0001$). ***E***, Diagram illustrating disruption of $Ca_V2.2^{CFP}/G\beta_1^{YFP}$ FRET in boutons of $1a^{-/-}$ neurons. One-way ANOVA analysis with *post hoc* Bonferroni's multiple comparison tests (***B***) and paired *t* test (***C***, ***D***) indicated significance. Error bars indicate SEM.

In contrast to $GB_{1a}/Ca_V2.2$ and $GB_{1a}/G\alpha_o$ interactions, agonist promoted FRET between $GB_{1a}/G\beta_1$ and $Ca_V2.2/G\beta_1$ proteins. Baclofen produced a ~30% increase in $GB_{1a}^{CFP}/G\beta_1^{YFP}$ FRET ($n = 14$–27, $p < 0.0001$) (Fig. 2*C*, left), and CGP54626 reduced FRET by ~48% ($n = 14$–17, $p < 0.0001$) (Fig. 2*C*, right). FRET efficiency between $Ca_V2.2^{CFP}$ and $G\beta_1^{YFP}$ proteins was increased by baclofen by ~32% ($n = 14$–15, $p < 0.0001$) (Fig. 2*D*, left), whereas it was decreased by CGP54626 antagonist by ~47% ($n = 16$–22, $p < 0.0001$) (Fig. 2*D*, right). These data indicate that basal GABA promotes $GB_{1a}/G\beta_1$ and $Ca_V2.2/G\beta_1$ associations in hippocampal boutons.

To test whether a reduction in FRET between $GB_{1a}/Ca_V2.2$ or between $GB_{1a}/G\alpha_o$ by GABA might be explained by receptor internalization, we used pHluorin, a pH-sensitive GFP, tagged to the N terminus of GB_{1a} protein to monitor surface expression of the GB_{1a} under physiological conditions. Fluorescence of pHluorin-GB_{1a} was unchanged by stimulation frequencies of 10 Hz or even 100 Hz spikes, or by maximal receptor activation (10 μM baclofen; Laviv et al., 2010) (Fig. 2*E*). These results suggest that reduction in the number of membrane receptors is unlikely to occur under our experimental conditions.

GB_{1a} is required for $G\beta\gamma/Ca_V2.2$ association

Having observed that binding of GABA to the GB_{1a} subunit is not essential for the precoupling of the $GB_{1a}R$ signaling complex, suggesting the formation of a receptor–G-protein–channel complex, we investigated whether the GB_{1a} protein is essential for $G\beta\gamma/Ca_V2.2$ interactions. Therefore, we measured possible FRET between $G\beta_1^{YFP}$ and $Ca_V2.2^{CFP}$ in boutons of hippocampal neurons prepared from GB_{1a} knock-out (Vigot et al., 2006) ($1a^{-/-}$) mice (Fig. 3*A*). Surprisingly, boutons lacking GB_{1a} protein revealed no specific FRET between $Ca_V2.2^{CFP}$ and $G\beta_1^{YFP}$ proteins under miniature synaptic activity (0.03 ± 0.004, $n = 31$) (Fig. 3*B*). Furthermore, neither block of synaptic activity nor agonist application induced specific FRET signals in $1a^{-/-}$ boutons ($n = 10$–18) (Fig. 3*B*). We also observed no specific FRET between $Ca_V2.2^{CFP}$ and either N-terminally tagged $G\gamma_2^{N'\text{-}YFP}$ (0.02 ± 0.01, $n = 10$) or C-terminally tagged $G\gamma_2^{C'\text{-}YFP}$ (0.03 ± 0.006, $n = 9$) G-proteins (Fig. 3*C*). By contrast, significant FRET ($p < 0.0001$) was observed between $G\gamma_2^{C'\text{-}YFP}/Ca_V2.2^{CFP}$ (0.12 ± 0.006, $n = 10$) and between $G\gamma_2^{N'\text{-}YFP}/Ca_V2.2^{CFP}$ (0.23 ± 0.005, $n = 15$) proteins in boutons of WT neurons, suggesting that there were no constraints on fluorophore mobility. Notably, $Ca_V2.2^{CFP}/G\beta_1^{N'\text{-}YFP}$ FRET was not altered in GB_{1b} knock-out ($1b^{-/-}$) boutons (0.18 ± 0.01, $n = 7$), consistent with the idea that GB_{1a} and not GB_{1b} is targeted to excitatory presynaptic boutons (Vigot et al., 2006). To confirm that FRET disruption was specific to the GB_{1a} deletion, we examined $Ca_V2.2^{CFP}/G\beta_1^{YFP}$ interactions following ectopic expression of GB_{1a} protein in $1a^{-/-}$ neurons. Indeed, expression of GB_{1a} protein rescued the $Ca_V2.2^{CFP}/G\beta_1^{YFP}$ FRET in $1a^{-/-}$ boutons (0.15 ± 0.01, $n = 17$) (Fig. 3*B*). Moreover, FRET between GB_2^{YFP} receptor subunit and $Ca_V2.2^{CFP}$ channel was abolished in $1a^{-/-}$ compared with WT neurons ($n = 8$, $p < 0.0001$) (Fig. 3*D*). Thus, deletion of the GB_{1a} protein disrupts association of key signaling molecules, $Ca_V2.2$ channel and $G\beta_1\gamma_2$ (Fig. 3*E*).

Proximal C-terminal GB_{1a} domain controls $G\beta\gamma$–$Ca_V2.2$ channel interaction

Next, we searched for the molecular domain in the GB_{1a} protein that mediates assembly of the $GB_{1a}R$–$G\beta\gamma$–$Ca_V2.2$ channel signaling complex. We created a series of GB_{1a} deletions/truncations and tested whether expression of genetically modified GB_{1a} versus wild-type GB_{1a} (GB_{1a}-WT) proteins in $1a^{-/-}$ neurons disrupts $Ca_V2.2^{CFP}/G\beta_1^{YFP}$ FRET. To rule out a possible role for the endogenous GB_{1a} subunit, we examined all of the truncations in the $1a^{-/-}$ cultures. First, we examined whether the GB_{1a} N-terminal sushi domains, functioning as axonal targeting signals (Biermann et al., 2010), mediate the $G\beta\gamma/Ca_V2.2$ interaction. Deletion of two sushi domains in the GB_{1a} (G28-Q157, GB_{1a}-ΔSD) (Fig. 4*A*) did not abolish $G\beta_1^{YFP}/Ca_V2.2^{CFP}$ FRET (0.13 ± 0.009, $n = 15$) (Fig. 4*B*). In addition, S269A mutation in the GB_{1a} protein (GB_{1a}-S269A), which was shown to decrease by >10-fold the affinity toward GABA (Galvez et al., 2000), resulted in $Ca_V2.2^{CFP}/G\beta_1^{YFP}$ FRET as well (0.13 ± 0.01, $n = 14$) (Fig. 4*B*). These results confirm our previous data showing significant FRET between $Ca_V2.2$ and $G\beta\gamma$ in the absence of GABA binding

(Fig. 1*D*,*E*) and suggest that agonist-induced activation of the receptor is not essential for the $Ca_V2.2/G\beta\gamma$ association.

Next, we tested whether the C terminus of GB_{1a} is responsible for the complex assembly. Truncation of the entire C terminus (at R857; GB_{1a}-Δ103) abolished $Ca_V2.2^{CFP}/G\beta_1^{YFP}$ FRET (0.024 ± 0.002, $n = 44$) (Fig. 4*B*). To precisely identify the site in GB_{1a} C terminus that mediates $Ca_V2.2/G\beta\gamma$ association, we created a series of C-terminal deletions/truncations: deletion of the proximal domain of C terminus (ΔR857-S877; GB_{1a}-Δ21), truncation at the coiled–coiled domain (K886; GB_{1a}-Δ74), and truncation of the distal part of C terminus (L921; GB_{1a}-Δ39). Notably, GB_{1a}-Δ21 abolished $Ca_V2.2^{CFP}/G\beta_1^{YFP}$ FRET (0.036 ± 0.007, $n = 24$) (Fig. 4*B*). In contrast, neither GB_{1a}-Δ74 nor GB_{1a}-Δ39 deletions prevented FRET between $G\beta_1^{YFP}$ and $Ca_V2.2^{CFP}$ (0.12 ± 0.02, $n = 14$; and 0.10 ± 0.01, $n = 17$, respectively). Together, these results suggest that the proximal C-terminal GB_{1a} domain is required for $G\beta\gamma$–$Ca_V2.2$ channel association at presynaptic boutons.

To assess whether the proximal C-terminal domain of GB_{1a} is essential for intermolecular associations between the receptor and $Ca_V2.2$ channel, we measured FRET between YFP-tagged GB_{1a}-WT or GB_{1a}-Δ21 with $Ca_V2.2^{CFP}$. The GB_{1a}-Δ21 deletion resulted in ~54% reduction of basal FRET (from 0.13 ± 0.02, $n = 20$, in GB_{1a}-WT to 0.06 ± 0.008, $n = 24$, $p < 0.001$) (Fig. 4*C*) and abolished baclofen-induced decrease of FRET, which is typically observed in GB_{1a}-WT (Fig. 4*C*). In contrast, deletion of the proximal C-terminal GB_{1a} domain did not affect either basal FRET between GB_{1a}-Δ21^{YFP} and $G\alpha_o^{CFP}$ or baclofen-induced FRET reduction ($n = 12$–16, $p < 0.05$) (Fig. 4*D*). These results suggest that the proximal C-terminal GB_{1a} domain mediates $GB_{1a}R$–$Ca_V2.2$ channel interaction, whereas it is dispensable for association of the GB_{1a} with $G\alpha_o$ G-protein subunit.

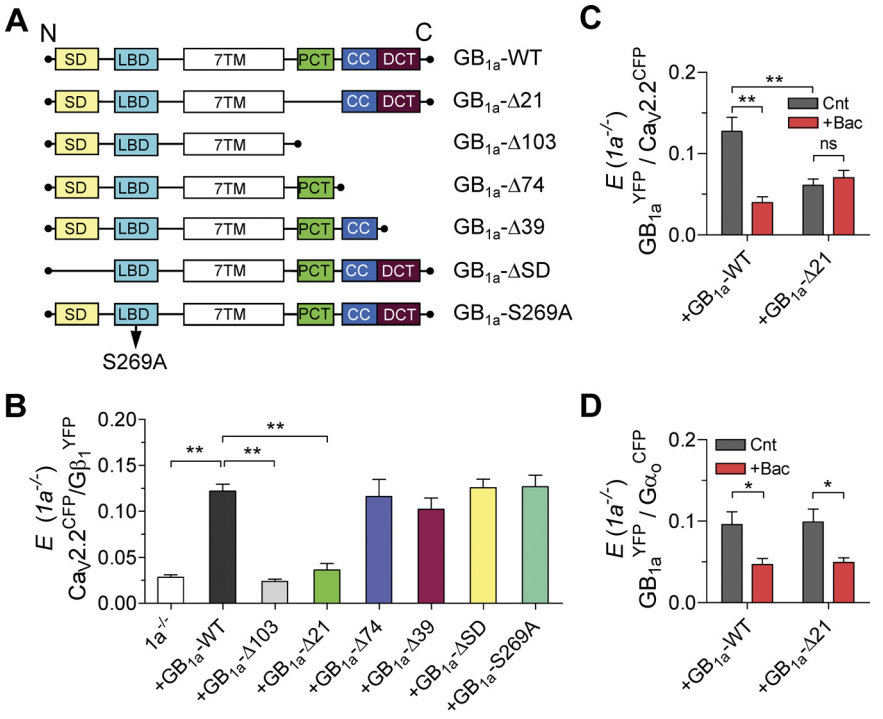

Figure 4. Proximal C-terminal domain of the GB_{1a} protein is essential for $G\beta\gamma/Ca_V2.2$ channel association. ***A***, Schematics show GB_{1a} constructs used to examine the domain responsible for $G\beta\gamma/Ca_V2.2$ association. SD, Two sushi domains; LBD, ligand-binding domain; 7TM, seven-transmembrane domain; PCT, proximal C-terminal domain; CC, coiled–coiled domain; DCT, distal C-terminal domain. ***B***, Mean FRET for the indicated transfection conditions in $1a^{-/-}$ neurons: GB_{1a}-WT ($n = 66, N = 11$), GB_{1a}-Δ103 ($n = 44, N = 8$, $^{**}p < 0.01$), GB_{1a}-Δ21 ($n = 24, N = 6$, $^{**}p < 0.0001$), GB_{1a}-Δ74 ($n = 14, N = 4, p > 0.05$), GB_{1a}-Δ39 ($n = 17, N = 4, p > 0.05$), GB_{1a}-ΔSD ($n = 15, N = 4, p > 0.05$), and GB_{1a}-S269A ($n = 14, N = 4, p > 0.05$). One-way ANOVA analysis with *post hoc* Dunnett's multiple-comparison tests relative to $1a^{-/-}$ boutons transfected with GB_{1a}-WT indicated significance. ***C***, Effect of 10 μM baclofen on the $GB_{1a}^{YFP}/Ca_V2.2^{CFP}$ FRET in $1a^{-/-}$ boutons transfected with GB_{1a}-WT ($n = 7$–20, $N = 3$–5, $^{**}p < 0.01$) or GB_{1a}-Δ21 ($n = 23$–24, $N = 5$–6, $p > 0.05$). ***D***, Effect of 10 μM baclofen on the $GB_{1a}^{YFP}/G\alpha_o^{CFP}$ FRET in $1a^{-/-}$ boutons transfected with GB_{1a}-WT ($n = 12$–15, $N = 3$–4, $^{*}p < 0.05$) or GB_{1a}-Δ21 ($n = 14$–16, $N = 3$–5, $^{*}p < 0.05$, paired *t* test). Error bars indicate SEM.

Proximal C-terminal GB_{1a} domain does not affect agonist-induced $GB_{1a}R$ activation and cAMP inhibition

Next, we explored whether proximal C-terminal GB_{1a} domain affects agonist-induced activation of the $GB_{1a}R$. Our previous work suggests that agonist-induced increase in FRET between the C-terminally tagged GB_{1a}/GB_2 receptor subunits reflects receptor activation (Laviv et al., 2010). Therefore, we measured the potency of baclofen to induce conformational changes in the GB_{1a}^{YFP}/GB_2^{CFP} receptor expressed in presynaptic boutons, comparing changes in receptors containing YFP-tagged GB_{1a}-WT versus GB_1a-Δ21 proteins. Baclofen dose–response curve for FRET efficiency between GB_{1a}^{CFP} and GB_2^{YFP} revealed no significant difference in ED_{50} between GB_{1a}-WT and GB_{1a}-Δ21 proteins (GB_{1a}-WT: 0.82 ± 0.003 μM, $n =$ 10–21; GB_1a-Δ21: 0.58 ± 0.05 μM, $n =$ 11–21) (Fig. 5*A*).

As deletion of the proximal C-terminal domain did not affect $GB_{1a}^{YFP}/G\alpha_o^{CFP}$ FRET, we assessed the ability of the GB_{1a}-Δ21 mutant to activate $G\alpha_{i/o}$ protein by measuring effect of baclofen on cAMP levels at individual synapses using CFP-Epac-YFP FRET reporter (van der Krogt et al., 2008). Baclofen induced ~50% increase in CFP-Epac-YFP FRET, indicating inhibition of cAMP level in GB_{1a}-WT-expressing boutons ($n = 30$–32, $p < 0.05$) (Fig. 5*B*). In contrast, baclofen did not affect CFP-Epac-YFP FRET in $1a^{-/-}$ boutons ($n = 25$–26, $p > 0.05$) (Fig. 5*B*). In GB_1a-Δ21-expressing boutons, baclofen induced a ~60% increase in FRET ($n = 27$–35, $p < 0.05$) (Fig. 5*B*). Together, these results suggest that the proximal C-terminal GB_{1a} domain does not affect agonist-induced $GB_{1a}R$ activation and $G\alpha_{i/o}$-dependent signaling.

Proximal C-terminal GB_{1a} domain is essential for agonist-induced presynaptic inhibition

Having established the necessity of GB_{1a} protein for $Ca_V2.2$–$G\beta\gamma$ association, we examined the functional role of the GB_{1a} protein and its proximal C-terminal domain in presynaptic inhibition of Ca^{2+} flux and synaptic vesicle release. First, we compared inhibitory effect of baclofen on presynaptic Ca^{2+} transients in functional boutons of $1a^{-/-}$ neurons versus boutons expressing GB_{1a}-WT or GB_{1a}-Δ21 proteins. Presynaptic Ca^{2+} transients evoked by low-frequency stimulation were measured by high-affinity fluorescent calcium indicator Oregon Green 488 BAPTA-1 AM (Laviv et al., 2010). Baclofen affected the size of action-potential-dependent fluorescence transients ($\Delta F/F$) in $1a^{-/-}$ boutons by 10 ± 1.7% ($n = 31$), and it induced significantly higher reduction of calcium transients in GB_{1a}-WT-expressing boutons (26.2 ± 1.7% inhibition, $n = 17$, $p < 0.001$)

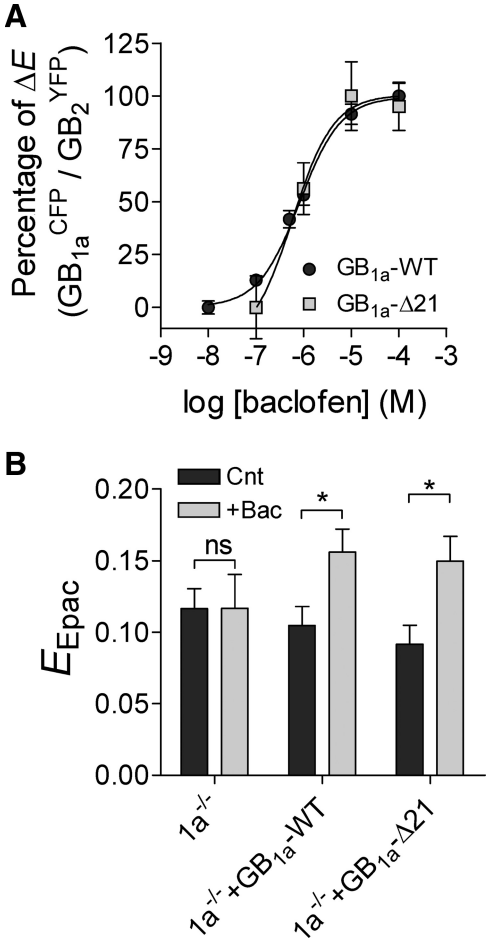

Figure 5. The GB_{1a} proximal C-terminal domain does not affect baclofen-induced GB_{1a}/GB_2 receptor activation and cAMP inhibition. ***A***, Dose–response curves of baclofen on GB_{1a}^{CFP}/GB_2^{YFP} FRET efficiency for GB_{1a}-WT ($n = 10–21$, $N = 5$, $ED_{50} = 0.82 \pm 0.003$ μM) and GB_{1a}-Δ21 ($n = 11–21$, $N = 3–5$, $ED_{50} = 0.58 \pm 0.013$ μM) proteins. *E* at 100 μM baclofen was set as 100%. ***B***, Effect of 10 μM baclofen on CFP–Epac–YFP FRET efficiency (E_{Epac}), reporting cAMP level, in $1a^{-/-}$ boutons and in $1a^{-/-}$ boutons expressing GB_{1a}-WT or GB_{1a}-Δ21 proteins. Baclofen increased E_{Epac} in GB_{1a}-WT-expressing ($n = 30–32$, $N = 6$, $^*p < 0.05$) and GB_{1a}-Δ21-expressing ($n = 27–35$, $N = 5–6$, $^*p < 0.05$) boutons, but did not affect E_{Epac} in $1a^{-/-}$ boutons ($n = 25–26$, $N = 5$, $p > 0.05$) One-way ANOVA with *post hoc* Bonferroni's multiple-comparison tests indicated significance. Error bars indicate SEM.

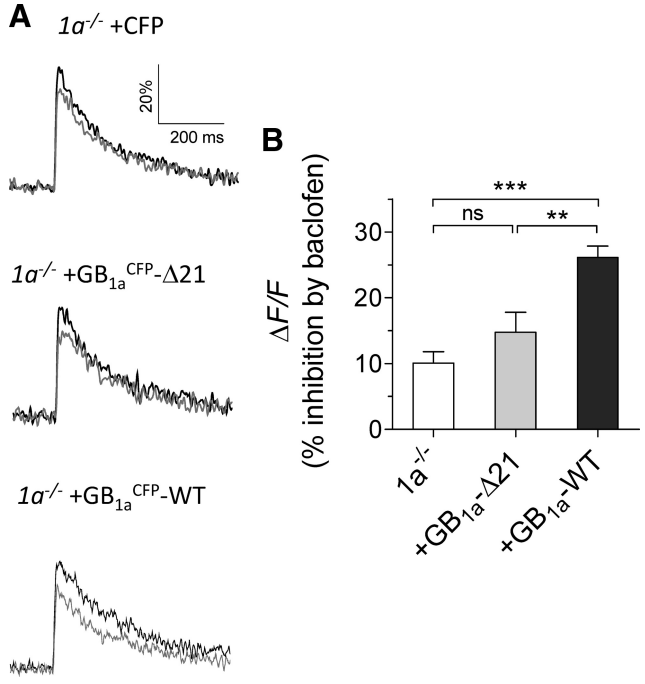

Figure 6. The role of the GB_{1a} proximal C-terminal domain on baclofen-induced inhibition of Ca^{2+} transients. ***A***, Baclofen did not affect spike-dependent presynaptic Ca^{2+} transients (Δ*F/F*) evoked by 0.2 Hz stimulation in $1a^{-/-}$ boutons and in GB_{1a}-Δ21-expressing boutons, but reduced it in GB_{1a}-WT-expressing boutons. Ca^{2+} transients were quantified as before (black) and after (gray) baclofen application (average of 10 traces). ***B***, Average data on baclofen-induced modification in Ca^{2+} transients in $1a^{-/-}$ ($n = 31$, $N = 6$, $p > 0.05$), GB_{1a}-WT-expressing ($n = 17$, $N = 4$, $^{***}p < 0.001$, compared with $1a^{-/-}$), and GB_{1a}-Δ21-expressing ($n = 19$, $N = 5$, $p > 0.05$, compared with $1a^{-/-}$) boutons. One-way ANOVA with *post hoc* Bonferroni's multiple-comparison tests indicated significance. Error bars indicate SEM.

(Fig. 6*A*,*B*). Notably, GB_{1a}-Δ21-expressing boutons displayed reduced sensitivity of Ca^{2+} transients to baclofen compared with GB_{1a}-WT-expressing boutons (14.8 ± 3% inhibition, $n = 19$, $p < 0.01$) (Fig. 6*A*,*B*), suggesting that baclofen-induced inhibition of N-type calcium channels depends on the proximal C-terminal domain of the GB_{1a} receptor subunit.

Next, we assessed the role of the proximal C-terminal GB_{1a} domain on baclofen-induced inhibition of synaptic vesicle exocytosis using FM4-64 dye (Laviv et al., 2010). The total pool of recycling vesicles was stained by maximal stimulation (600 APs at 10 Hz) and subsequently destained by 1 Hz stimulation. Baclofen (10 μM) profoundly decreased the destaining rate constant (measured as $1/\tau_{decay}$, whereas τ_{decay} is an exponential time course) in WT ($N = 12$, $p < 0.001$) (Fig. 7*A*,*F*), but it affected the destaining rate by a much lesser extent in WT neurons expressing membrane-targeted Gβγ scavenger, N-myristoylated phosducin (Rishal et al., 2005) (*Myr*Phd, $N = 4$, $p < 0.001$) (Fig. 7*B*,*F*). Furthermore, baclofen did not affect the destaining rate in $1a^{-/-}$ ($N = 9$, $p > 0.3$) (Fig. 7*C*,*F*) boutons, complementing electrophysiological data on the lack of baclofen effect on basal synaptic transmission in $1a^{-/-}$ CA3-CA1 synapses (Vigot et al., 2006). Transient expression of GB_{1a}-WT protein together with GFP in $1a^{-/-}$ neurons resulted in recovery of the inhibitory effect of baclofen ($N = 6$, $p < 0.001$, compared with GFP-expressing neurons) (Fig. 7*D*,*F*). Moreover, transient expression of the GB_{1a}-Δ21 together with GFP in $1a^{-/-}$ neurons significantly reduced baclofen effect on the destaining rate constant ($N = 6$, $p < 0.0001$, compared with expression of GB_{1a}–WT + GFP-in $1a^{-/-}$ neurons) (Fig. 7*E*,*F*). These results strongly suggest that (1) the GB_{1a} protein is essential for baclofen-induced inhibition of synaptic vesicle release, (2) Gβγ is a mediator of baclofen-induced presynaptic inhibition, and (3) the proximal C-terminal GB_{1a} domain is essential for baclofen-induced inhibition of synaptic vesicle release in hippocampal boutons.

Discussion

In the current study, we discovered that the $GABA_{B1a}$ subunit plays a crucial role in creating a functional receptor–G-protein–channel complex in presynaptic boutons of hippocampal neurons. First, we found that the presynaptic GB_{1a}R, heterotrimeric G_o-protein and $Ca_V2.2$ channel are precoupled, forming macromolecular complex regardless of synaptic activity and agonist stimulation at individual hippocampal boutons. Second, basal GABA levels are sufficient to induce rearrangements within the complex. Third, intermolecular associations within the receptor, Gβγ, and $Ca_V2.2$ channel complex require expression of the GB_{1a} protein. Fourth, we identified the proximal C-terminal domain in the GB_{1a} protein as essential motif for the complex formation. This

domain is required specifically for baclofen-induced presynaptic inhibition of Ca^{2+} transients and vesicle release, but not for the receptor activation and cAMP inhibition. Together, these findings suggest that compartmentalization of the presynaptic signaling complex, in addition to agonist-induced receptor activation, critically controls the $GB_{1a}R$-mediated presynaptic inhibition at hippocampal boutons.

Presynaptic $GABA_BR$–G-protein–$Ca_V2.2$ channel signaling complex

Intermolecular interactions between receptors, G-proteins, and high-voltage-gated Ca^{2+} channels represent key events in inhibition of neurotransmitter release. Accumulating biochemical and electrophysiological evidence suggests that direct membrane-delimited interaction of Ca^{2+} channel α_1 subunit with $G\beta\gamma$ mediates inhibition of presynaptic calcium currents and of synaptic vesicle exocytosis by GPCRs (Dascal, 2001; Dolphin, 2003; Tedford and Zamponi, 2006; Catterall and Few, 2008). Yet, the mechanisms of intermolecular coupling remain controversial. Although "physical scaffolding" of signaling components within the same G-protein-coupled signaling unit has been proposed to enhance signaling specificity (Neubig, 1994; Tsunoda et al., 1997), direct evidence for compartmentalization of GPCR signaling at central synapses is still missing.

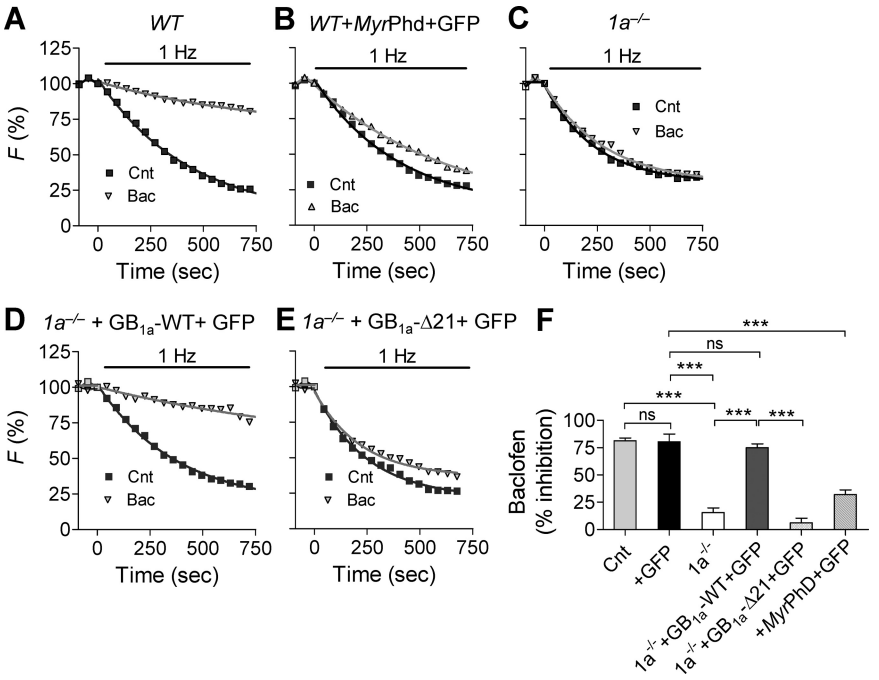

Figure 7. The GB_{1a} proximal C-terminal domain is required for baclofen-induced inhibition of synaptic vesicle release. ***A–E***, Representative FM destaining curves before and after application of 10 μM baclofen in WT cultures ($n = 84$, ***A***), WT cultures transfected with *Myr*Phd and GFP ($n = 112$, ***B***), $1a^{-/-}$ cultures ($n = 71$, ***C***), $1a^{-/-}$ cultures transfected with GB_{1a}-WT and GFP ($n = 69$, ***D***), and $1a^{-/-}$ cultures transfected with GB_{1a}-Δ21 and GFP ($n = 94$, ***E***). ***F***, Summary of baclofen effect on FM destaining rate in WT ($N = 12$), GFP-expressing boutons ($N = 3$), WT cultures transfected with *Myr*Phd and GFP ($N = 4$), $1a^{-/-}$ ($N = 9$), $1a^{-/-}$ transfected with GB_{1a}-WT and GFP ($N = 6$), and $1a^{-/-}$ transfected with GB_{1a}-Δ21 and GFP ($N = 6$) cultures. Error bars indicate SEM. (***$p < 0.001$, n.s. for $p > 0.05$, one-way ANOVA analysis with *post hoc* Bonferroni's multiple-comparison tests).

To explore the microarchitecture and dynamics of proteins in specialized presynaptic compartments, FRET spectroscopy has been used. Our data provide direct evidence for the close (<100 Å) proximity between the tagged $GB_{1a}R$, $G\alpha_o\beta_1\gamma_2$ G-protein heterotrimer, and $Ca_V2.2$ channel (Fig. 1). Specific FRET signals were detected in boutons lacking SNARE-mediated exocytosis, under block of receptor activation by antagonist, and in boutons expressing mutated GB_{1a}-S269A protein with reduced affinity for GABA. These FRET-based data resonate with the recent proteomic study on molecular nano-environment of the Ca_V2 channels in the rodent brain (Müller et al., 2010). The authors demonstrated direct interaction between the $GABA_B$ receptor subunits and $Ca_V2.2$ channel under high stringency conditions. However, lack of interaction between the $GABA_B$ receptor and $Ca_V2.2$ channel was observed under resting conditions by coimmunoprecipitation in sensory dorsal root ganglion neurons (Puckerin et al., 2006), suggesting possible differences in signaling complex organization at central versus peripheral synapses. Furthermore, a direct interaction between $Ca_V2.2$ and $G\beta\gamma$ G-protein subunits in the CNS has been also demonstrated by proteomic studies (Khanna et al., 2007; Müller et al., 2010). Together, FRET-based and proteomic analyses strongly suggest assembly of the $GABA_B$ receptor presynaptic signaling complexes under resting conditions in central synapses.

What is the molecular mechanism underling the $GB_{1a}R$-mediated presynaptic inhibition at hippocampal synapses? One possibility is that presynaptic inhibition arises from reduction in the number of available signaling molecules at the plasma membrane of boutons. For example, agonist-induced cointernalization of $Ca_V2.2$ channel with GPCRs such as opioid-like-receptor ORL1 and dopamine D1 receptor have been observed in earlier studies (Altier et al., 2006; Altier and Zamponi, 2008; Kisilevsky et al., 2008). To test whether the membrane fraction of $GB_{1a}Rs$ depends on activity-dependent concentration of GABA in the vicinity of boutons, we measured fluorescence of pHluorin, N-terminally tagged to the GB_{1a} protein as function of neuronal activity or agonist stimulation. We did not observe any change in the pHluorin fluorescence as function of stimulation frequency or agonist concentration (Fig. 2*E*), suggesting that under physiological conditions, reduction in the number of $GB_{1a}Rs$ at the presynaptic membrane does not contribute to presynaptic inhibition at hippocampal boutons. In addition, agonist-induced, receptor-independent internalization of $Ca_V2.2$ channel might mediate presynaptic inhibition as has been suggested in dorsal root ganglion neurons (Tombler et al., 2006). However, this mechanism seems to be $G\beta\gamma$-independent, and our results suggest that the $GB_{1a}R$-mediated presynaptic inhibition in hippocampal synapses is mediated by $G\beta\gamma$ (Fig. 7*F*).

Our data favor the model based on agonist-induced structural rearrangements within the $GB_{1a}R$–$G\beta\gamma$–$Ca_V2.2$ channel complex as the mechanism mediating inhibition of basal synaptic vesicle exocytosis. Although synaptic activity was not essential for the complex formation, quantal synaptic transmission, an elementary unit of synaptic communication, induced structural rearrangements between the presynaptic signaling units (Fig. 2). Tonic activation of the $GB_{1a}R$ complex under miniature synaptic activity (in the presence of TTX) was relieved following application of the receptor antagonist. Thus, basal levels of GABA in the synaptic cleft are sufficient to activate $GB_{1a}Rs$ through induction of conformation changes in the GB_{1a}/GB_2 heterodimer (Laviv et

al., 2010), leading to activation of G-protein and closer association of precoupled $G\beta\gamma$ subunits and $Ca_V2.2$ channels (Fig. 2*G*). As a result of these conformational rearrangements, basal GABA induces reduction of presynaptic calcium flux (Fig. 6) and consequent inhibition of synaptic vesicle release in hippocampal boutons (Fig. 7).

Proximal GB_{1a} C-terminal domain is required for the $GB_{1a}R$ complex formation

It first came as a surprise that FRET between $Ca_V2.2/G\beta\gamma$ was reduced to background level in $1a^{-/-}$ boutons lacking GB_{1a} protein (Fig. 3). Presynaptic expression of the tagged $Ca_V2.2$ channels and $G\beta\gamma$ subunits was not altered in $1a^{-/-}$ neurons, suggesting a proper trafficking to the $1a^{-/-}$ boutons. The lack of specific FRET was observed with both $G\beta_1$ and $G\gamma_2$ proteins and did not depend on the position of fluorophore tagging, suggesting that there were no constraints on fluorophore mobility that could convert changes in orientation into substantial changes in FRET. Therefore, these results suggest that reduction in donor–acceptor distance, rather than dipole–dipole orientation of the donor and acceptor fluorophores, underlies FRET disruption. Neither alterations in synaptic activity nor agonist-induced stimulation triggered the complex formation. This association was recovered following transient expression of the GB_{1a}-WT protein in $1a^{-/-}$ neurons. Notably, partial rescue of $Ca_V2.2/G\beta\gamma$ association was observed following expression of the GB_{1a}-S269A protein with >10-fold reduced affinity to GABA (Galvez et al., 2000). These results led to the conclusion that the GB_{1a} protein is essential for precoupling of the receptor, $G\beta\gamma$, and $Ca_V2.2$ channel.

What is the GB_{1a} molecular domain mediating formation of the $GB_{1a}R$ signaling complex at hippocampal boutons? Previous work suggested that the C terminus of the GB_1 receptor subunit is not essential for the $GABA_B$ receptor activation detected through GIRK channel activity (Margeta-Mitrovic et al., 2001). Based on these results, the authors concluded that the GB_1 protein is not required for specific coupling to G-protein and its activation. Our findings confirm that C terminus of the GB_{1a} protein is not required for activation of the receptor, receptor/$G\alpha_{i/o}$ interaction, and cAMP inhibition. Conversely, our data strongly suggest that the GB_{1a} proximal C-terminal domain (R857-S877) is required for a tight association between the receptor, $G\beta\gamma$, and $Ca_V2.2$ channel. Functionally, deletion of this GB_{1a} domain impaired presynaptic inhibition of Ca^{2+} flux and of synaptic vesicle exocytosis. These results imply differential regulation of GIRK and $Ca_V2.2$ channels by the GB_{1a} C terminus. Thus, in addition to agonist-induced receptor activation, preassembly of the $GB_{1a}R$–$G\beta\gamma$–$Ca_V2.2$ channel signaling complex is essential for agonist-induced presynaptic inhibition at hippocampal boutons. It will be interesting to explore functional significance of GB_1 proximal C-terminal domain on regulation of voltage-gated Ca^{2+} channels and NMDA receptors in spines and dendrites (Chalifoux and Carter, 2010, 2011).

Does association of $G\beta\gamma$ and $Ca_V2.2$ channel result from constitutive activity of $GB_{1a}Rs$ expressed at hippocampal boutons? Unfortunately, no information is available on constitutive activity of presynaptic $GB_{1a}Rs$ in central synapses. Our data provide no evidence for constitutive $GB_{1a}R$ activity because CGP54626 antagonist, which works as a partial agonist at constitutively active $GABA_BRs$ (Mukherjee et al., 2006), did not affect any tested association between the $GB_{1a}R$, $G\beta\gamma$ subunits, and $Ca_V2.2$ channel in the absence of GABA (data not shown). Therefore, our results imply that GB_{1a} plays an essential role in coordinating and integrating the complex assembly regardless of agonist-induced receptor activation.

Individual hippocampal boutons may express diverse GPCRs, in addition to GB_{1a}/GB_2 receptors, raising the question of the mechanisms of GPCR-mediated signaling in $1a^{-/-}$ boutons lacking functional $G\beta_1\gamma_2/Ca_V2.2$ signaling complexes. Presynaptic inhibition mediated through adenosine (Vigot et al., 2006) and muscarinic (Vertkin and Slutsky, unpublished data) receptors remains functional in $1a^{-/-}$ hippocampal synapses. These data imply that adenosine and muscarinic receptors are capable of presynaptic inhibition through distinct Ca^{2+}-dependent and Ca^{2+}-independent mechanisms. For example, adenosine-induced presynaptic inhibition is not limited to the N-type calcium channel (Wu and Saggau, 1994; Dittman and Regehr, 1996). Moreover, M_2 muscarinic receptors can inhibit neurotransmitter release through direct block of release machinery (Parnas and Parnas, 2007). Further work is needed to understand the precise mechanisms underlying signaling specificity at synapses expressing multiple GPCRs.

Together, our data support the "physical scaffolding" model of GPCR, G-protein, and effector suggesting a precoupling of presynaptic G-protein signaling complexes in central synapses. Our study revealed the proximal C-terminal part of GB_{1a} receptor subunit as essential domain for a tight association of the receptor, $G\beta\gamma$ subunits, and $Ca_V2.2$ channel. As the GB_{1a} proximal C-terminal domain does not affect receptor activation, identification of this motif allowed us, for the first time, to isolate functional significance underlying precoupling of signaling units in a macromolecular complex. It remains to be seen whether compartmentalization of GPCRs, $G\beta\gamma$ subunits, and $Ca_V2.2/1$ channels constitutes a general mechanism underlying presynaptic inhibition at central synapses.

References

Abramov E, Dolev I, Fogel H, Ciccotosto GD, Ruff E, Slutsky I (2009) Amyloid-[beta] as a positive endogenous regulator of release probability at hippocampal synapses. Nat Neurosci 12:1567–1576.

Altier C, Zamponi GW (2008) Signaling complexes of voltage-gated calcium channels and G-protein-coupled receptors. J Recept Signal Transduct Res 28:71–81.

Altier C, Khosravani H, Evans RM, Hameed S, Peloquin JB, Vartian BA, Chen L, Beedle AM, Ferguson SS, Mezghrani A, Dubel SJ, Bourinet E, McRory JE, Zamponi GW (2006) ORL1 receptor-mediated internalization of N-type calcium channels. Nat Neurosci 9:31–40.

Bettler B, Kaupmann K, Mosbacher J, Gassmann M (2004) Molecular structure and physiological functions of GABAB receptors. Physiol Rev 84:835–867.

Biermann B, Ivankova-Susankova K, Bradaia A, Abdel Aziz S, Besseyrias V, Kapfhammer JP, Missler M, Gassmann M, Bettler B (2010) The sushi domains of GABAB receptors function as axonal targeting signals. J Neurosci 30:1385–1394.

Boyer SB, Clancy SM, Terunuma M, Revilla-Sanchez R, Thomas SM, Moss SJ, Slesinger PA (2009) Direct interaction of GABAB receptors with M_2 muscarinic receptors enhances muscarinic signaling. J Neurosci 29:15796–15809.

Catterall WA (2000) Structure and regulation of voltage-gated Ca^{2+} channels. Annu Rev Cell Dev Biol 16:521–555.

Catterall WA, Few AP (2008) Calcium channel regulation and presynaptic plasticity. Neuron 59:882–901.

Chalifoux JR, Carter AG (2010) GABAB receptors modulate NMDA receptor calcium signals in dendritic spines. Neuron 66:101–113.

Chalifoux JR, Carter AG (2011) GABAB receptor modulation of voltage-sensitive calcium channels in spines and dendrites. J Neurosci 31:4221–4232.

Dascal N (2001) Ion-channel regulation by G proteins. Trends Endocrinol Metab 12:391–398.

De Waard M, Hering J, Weiss N, Feltz A (2005) How do G proteins directly control neuronal Ca^{2+} channel function? Trends Pharmacol Sci 26:427–436.

Dittman JS, Regehr WG (1996) Contributions of calcium-dependent and calcium-independent mechanisms to presynaptic inhibition at a cerebellar synapse. J Neurosci 16:1623–1633.

Dolphin AC (2003) G protein modulation of voltage-gated calcium channels. Pharmacol Rev 55:607–627.

Dunlap K, Fischbach GD (1978) Neurotransmitters decrease the calcium ocmponent of sensory neurone action potentials. Nature 276:837–839.

Dunlap K, Luebke JI, Turner TJ (1995) Exocytotic Ca^{2+} channels in mammalian central neurons. Trends Neurosci 18:89–98.

Fowler CE, Aryal P, Suen KF, Slesinger PA (2007) Evidence for association of GABA(B) receptors with Kir3 channels and regulators of G protein signalling (RGS4) proteins. J Physiol 580:51–65.

Frank M, Thümer L, Lohse MJ, Bünemann M (2005) G protein activation without subunit dissociation depends on a G{alpha}(i)-specific region. J Biol Chem 280:24584–24590.

Galés C, Van Durm JJ, Schaak S, Pontier S, Percherancier Y, Audet M, Paris H, Bouvier M (2006) Probing the activation-promoted structural rearrangements in preassembled receptor–G protein complexes. Nat Struct Mol Biol 13:778–786.

Galvez T, Urwyler S, Prézeau L, Mosbacher J, Joly C, Malitschek B, Heid J, Brabet I, Froestl W, Bettler B, Kaupmann K, Pin JP (2000) Ca^{2+} requirement for high-affinity gamma-aminobutyric acid (GABA) binding at GABAB receptors: involvement of serine 269 of the GABABR1 subunit. Mol Pharmacol 57:419–426.

Guetg N, Seddik R, Vigot R, Turecek R, Gassmann M, Vogt KE, Bräuner-Osborne H, Shigemoto R, Kretz O, Frotscher M, Kulik A, Bettler B (2009) The $GABA_{B1a}$ isoform mediates heterosynaptic depression at hippocampal mossy fiber synapses. J Neurosci 29:1414–1423.

Hein P, Frank M, Hoffmann C, Lohse MJ, Bünemann M (2005) Dynamics of receptor/G protein coupling in living cells. EMBO J 24:4106–4114.

Hille B (1994) Modulation of ion-channel function by G-protein-coupled receptors. Trends Neurosci 17:531–536.

Jones KA, Borowsky B, Tamm JA, Craig DA, Durkin MM, Dai M, Yao WJ, Johnson M, Gunwaldsen C, Huang LY, Tang C, Shen Q, Salon JA, Morse K, Laz T, Smith KE, Nagarathnam D, Noble SA, Branchek TA, Gerald C (1998) GABA(B) receptors function as a heteromeric assembly of the subunits GABA(B)R1 and GABA(B)R2. Nature 396:674–679.

Kaupmann K, Malitschek B, Schuler V, Heid J, Froestl W, Beck P, Mosbacher J, Bischoff S, Kulik A, Shigemoto R, Karschin A, Bettler B (1998) GABA(B)-receptor subtypes assemble into functional heteromeric complexes. Nature 396:683–687.

Khanna R, Zougman A, Stanley EF (2007) A proteomic screen for presynaptic terminal N-type calcium channel (CaV2.2) binding partners. J Biochem Mol Biol 40:302–314.

Kisilevsky AE, Mulligan SJ, Altier C, Iftinca MC, Varela D, Tai C, Chen L, Hameed S, Hamid J, Macvicar BA, Zamponi GW (2008) D1 receptors physically interact with N-type calcium channels to regulate channel distribution and dendritic calcium entry. Neuron 58:557–570.

Kuner R, Köhr G, Grünewald S, Eisenhardt G, Bach A, Kornau HC (1999) Role of heteromer formation in GABAB receptor function. Science 283:74–77.

Laviv T, Riven I, Dolev I, Vertkin I, Balana B, Slesinger PA, Slutsky I (2010) Basal GABA regulates GABA(B)R conformation and release probability at single hippocampal synapses. Neuron 67:253–267.

Lohse MJ, Nikolaev VO, Hein P, Hoffmann C, Vilardaga JP, Bünemann M (2008) Optical techniques to analyze real-time activation and signaling of G-protein-coupled receptors. Trends Pharmacol Sci 29:159–165.

Margeta-Mitrovic M, Jan YN, Jan LY (2001) Function of GB1 and GB2 subunits in G protein coupling of GABA(B) receptors. Proc Natl Acad Sci U S A 98:14649–14654.

Mukherjee RS, McBride EW, Beinborn M, Dunlap K, Kopin AS (2006) Point mutations in either subunit of the GABAB receptor confer constitutive activity to the heterodimer. Mol Pharmacol 70:1406–1413.

Müller CS, Haupt A, Bildl W, Schindler J, Knaus HG, Meissner M, Rammner B, Striessnig J, Flockerzi V, Fakler B, Schulte U (2010) Quantitative proteomics of the Cav2 channel nano-environments in the mammalian brain. Proc Natl Acad Sci U S A 107:14950–14957.

Neubig RR (1994) Membrane organization in G-protein mechanisms. FASEB J 8:939–946.

Neubig RR, Gantzos RD, Thomsen WJ (1988) Mechanism of agonist and antagonist binding to alpha 2 adrenergic receptors: evidence for a precoupled receptor–guanine nucleotide protein complex. Biochemistry 27:2374–2384.

Nobles M, Benians A, Tinker A (2005) Heterotrimeric G proteins precouple with G protein-coupled receptors in living cells. Proc Natl Acad Sci U S A 102:18706–18711.

Nowycky MC, Fox AP, Tsien RW (1985) Three types of neuronal calcium channel with different calcium agonist sensitivity. Nature 316:440–443.

Orly J, Schramm M (1976) Coupling of catecholamine receptor from one cell with adenylate cyclase from another cell by cell fusion. Proc Natl Acad Sci U S A 73:4410–4414.

Parnas H, Parnas I (2007) The chemical synapse goes electric: Ca^{2+}- and voltage-sensitive GPCRs control neurotransmitter release. Trends Neurosci 30:54–61.

Parnas H, Segel L, Dudel J, Parnas I (2000) Autoreceptors, membrane potential and the regulation of transmitter release. Trends Neurosci 23:60–68.

Puckerin A, Liu L, Permaul N, Carman P, Lee J, Diversé-Pierluissi MA (2006) Arrestin is required for agonist-induced trafficking of voltage-dependent calcium channels. J Biol Chem 281:31131–31141.

Rishal I, Porozov Y, Yakubovich D, Varon D, Dascal N (2005) $G-^{2}-^{3}$-dependent and $G-^{2}-^{3}$-independent basal activity of G protein-activated K+ channels. J Biol Chem 280:16685–16694.

Riven I, Iwanir S, Reuveny E (2006) GIRK channel activation involves a local rearrangement of a preformed G protein channel complex. Neuron 51:561–573.

Sakaba T, Neher E (2003) Direct modulation of synaptic vesicle priming by GABA(B) receptor activation at a glutamatergic synapse. Nature 424:775–778.

Scanziani M, Capogna M, Gähwiler BH, Thompson SM (1992) Presynaptic inhibition of miniature excitatory synaptic currents by baclofen and adenosine in the hippocampus. Neuron 9:919–927.

Schwenk J, Metz M, Zolles G, Turecek R, Fritzius T, Bildl W, Tarusawa E, Kulik A, Unger A, Ivankova K, Seddik R, Tiao JY, Rajalu M, Trojanova J, Rohde V, Gassmann M, Schulte U, Fakler B, Bettler B (2010) Native GABA(B) receptors are heteromultimers with a family of auxiliary subunits. Nature 465:231–235.

Slutsky I, Sadeghpour S, Li B, Liu G (2004) Enhancement of synaptic plasticity through chronically reduced Ca^{2+} flux during uncorrelated activity. Neuron 44:835–849.

Takahashi T, Kajikawa Y, Tsujimoto T (1998) G-protein-coupled modulation of presynaptic calcium currents and transmitter release by a GABAB receptor. J Neurosci 18:3138–3146.

Tedford HW, Zamponi GW (2006) Direct G protein modulation of Ca_v2 calcium channels. Pharmacol Rev 58:837–862.

Tolkovsky AM, Levitzki A (1978) Mode of coupling between the beta-adrenergic receptor and adenylate cyclase in turkey erythrocytes. Biochemistry 17:3795.

Tombler E, Cabanilla NJ, Carman P, Permaul N, Hall JJ, Richman RW, Lee J, Rodriguez J, Felsenfeld DP, Hennigan RF, Diversé-Pierluissi MA (2006) G protein-induced trafficking of voltage-dependent calcium channels. J Biol Chem 281:1827–1839.

Tsunoda S, Sierralta J, Sun Y, Bodner R, Suzuki E, Becker A, Socolich M, Zuker CS (1997) A multivalent PDZ-domain protein assembles signalling complexes in a G-protein-coupled cascade. Nature 388:243–249.

van der Krogt GN, Ogink J, Ponsioen B, Jalink K (2008) A comparison of donor–acceptor pairs for genetically encoded FRET sensors: application to the Epac cAMP sensor as an example. PLoS One 3:e1916.

Vigot R, Barbieri S, Bräuner-Osborne H, Turecek R, Shigemoto R, Zhang YP, Luján R, Jacobson LH, Biermann B, Fritschy JM, Vacher CM, Müller M, Sansig G, Guetg N, Cryan JF, Kaupmann K, Gassmann M, Oertner TG, Bettler B (2006) Differential compartmentalization and distinct functions of GABAB receptor variants. Neuron 50:589–601.

White JH, Wise A, Main MJ, Green A, Fraser NJ, Disney GH, Barnes AA, Emson P, Foord SM, Marshall FH (1998) Heterodimerization is required for the formation of a functional GABA(B) receptor. Nature 396:679–682.

Wu LG, Saggau P (1994) Adenosine inhibits evoked synaptic transmission primarily by reducing presynaptic calcium influx in area CA1 of hippocampus. Neuron 12:1139–1148.

Wu LG, Saggau P (1995) GABAB receptor-mediated presynaptic inhibition in guinea-pig hippocampus is caused by reduction of presynaptic Ca^{2+} influx. J Physiol 485(Pt 3):649–657.

Wu LG, Saggau P (1997) Presynaptic inhibition of elicited neurotransmitter release. Trends Neurosci 20:204–212.

Zamponi GW, Snutch TP (1998) Modulation of voltage-dependent calcium channels by G proteins. Curr Opin Neurobiol 8:351–356.